

On the locked dynamical states of an overdamped Josephson junction array

This article has been downloaded from IOPscience. Please scroll down to see the full text article.

1996 J. Phys.: Condens. Matter 8 3057

(<http://iopscience.iop.org/0953-8984/8/17/016>)

View [the table of contents for this issue](#), or go to the [journal homepage](#) for more

Download details:

IP Address: 171.66.16.208

The article was downloaded on 13/05/2010 at 16:34

Please note that [terms and conditions apply](#).

On the locked dynamical states of an overdamped Josephson junction array

J C Ciria[†] and C Giovannella[‡]

[†] Dipartimento di Fisica dell'Università di Roma, Tor Vergata, Via della Ricerca Scientifica 1, I-00133 Roma, Italy

[‡] Sezione INFN and Sezione INFN dell'Università di Roma, Tor Vergata, Via della Ricerca Scientifica 1, I-00133 Roma, Italy

Received 3 August 1995, in final form 13 December 1995

Abstract. We study the dynamics of a 2D array of Josephson junctions biased with both dc and ac currents. Within certain ranges of the dc current intensity a locking between the natural oscillation frequency of the array and that of the ac forcing term occurs, giving rise to periodic solutions. As expected, a set of Shapiro steps appears in the $\langle V \rangle$ - I curve. We show that there is no one-to-one correspondence between the value of $\langle V \rangle$ on the Shapiro step and the dynamical state of the array. In particular for a frustration equal to 0.5, besides the well-known ground state, g.s., of the array (the checkerboard-like vortex configuration), there exist other dynamical states accessible to the system. These latter are characterized by the same average voltage of the g.s. but different average energies and vortex configurations, with one or more domain walls. These 'new' states are stable against small thermal fluctuations and phase perturbations. A better insight into the physical conditions needed to generate them has been obtained by studying the dynamical behaviour of a ladder as a function of its size and of its orientation with respect to the external bias current. The relevance of our observations to the experimental studies of the array dynamics performed on a microscopical scale is briefly discussed.

1. Introduction

One of the most remarkable facts in the dynamical behaviour of the arrays of superconducting junctions (SJA) is the appearance of Shapiro steps (SS) when these networks are biased with both ac and dc currents [1, 2, 3]. The development of the SS can be well understood within the framework of the model describing the coupling between two oscillators. They mirror the existence of a locking between the external current and the intrinsic frequency of the system [4, 5].

Integer giant Shapiro steps (GSS), appearing at voltage $\langle V \rangle = nN_y h\nu/2e$ (where ν is the frequency of the ac current, N_y the number of junctions along the direction of the bias current and n any integer number), are trivial generalizations of the Shapiro steps found in a single junction. The observation of GSS implies that inside the sample the current flows only along the direction of the incoming bias current, showing a perfect symmetry along the axis perpendicular to this direction.

If by any means this symmetry is broken, a locking on non-trivial dynamical states becomes possible, as is evident from the appearance of half-integer or subharmonic Shapiro steps (SSS) [2, 6]. It may be caused, in fact, by the introduction of any type of disorder (coupling, positional, etc), by an inhomogeneous current polarization or, finally, by the presence of an external magnetic field. In this latter case, a devil's staircase structure with a

fractal dimension $D = 0.88$ [5] has been observed. Under these conditions the array cannot be reduced any longer to a parallel arrangement of one-dimensional columns of oscillators, and the 2D cooperative behaviour comes into play.

Usually, the SSS are explained in terms of the formation and the coherent displacement of superarrays of vortices commensurate to the dimension of the array [8, 9]. This interpretation, however, is somewhat contradicted by numerical simulations dealing with the dynamical behaviour of a single plaquette [10], of a ladder [11] and of small square arrays [5], which show locked states at fractional values of the normalized voltage that would correspond to commensurate arrays of vortices with a lattice period larger than that of the simulated SJA.

Another common assumption is that the width of the SS is related to the extension of the attraction basin of a certain dynamical state. From that and from the fact that the value of the SS average voltage does not depend on the initial distribution of the phases [9], one is induced to extrapolate a one-to-one correspondence between the vortex configuration of the locked dynamical state and the value of the SS average voltage. As far as real experiments are concerned this would imply that the sample should always be attracted by the same dynamical basin, whatever the orientation of the phases is at the temperature where they start to couple coherently. It is well known that control of the phase orientation in the proximity of the freezing temperature is not easy, and it is not obvious that the final state would not depend, for example, on the cooling rate, on the intensity of the self-field and so on. Although the temperature fluctuations may help in finding the dynamical ground state and, in some cases, in destroying metastable states, trapping by ‘localized’ attractors is not, in fact, such an exotic eventuality.

In this paper we submit the above assumptions to a deep scrutiny and we show that the monitoring of quantities like the Josephson energy of the array (defined in section 3) is essential if one is to obtain a deeper insight into the dynamical phase space of the SJA. The work presented here may be relevant to the interpretation of experiments devoted to monitoring the vortex dynamics in 2D arrays and in ladders of superconducting junctions. Moreover it may help also to explain the operation of those superconducting devices that are based on a coherent vortex dynamics.

This paper is organized as follows. In section 2 we describe the model that we employed. In section 3 we show that the dynamical state of the system (identified, for example, by the vortex configuration) cannot be unequivocally defined by quantities like the average voltage and/or the width of a Shapiro step. In particular we show that, depending on the initial conditions, several dynamical states are accessible to the array within a unique voltage plateau. We present also a check of the stability of these states against temperature and small perturbations. Finally, section 4 is devoted to the study of the influence of the lattice geometry on the dynamical properties of the array and in particular on the appearance of the dynamical states described in the previous sections.

2. The model

We have simulated the dynamics of an array of overdamped Josephson junctions in the limit of zero shunt capacity and negligible inductance. We also assume that the phase of the order parameter Φ_i is constant on each grain (i.e. we consider point grains). The dynamical equation for site i is [12]

$$\sum_{ij} \left(\frac{V_{ij}}{R_{ij}} + I_c \sin(\Phi_i - \Phi_j - A_{ij}) \right) = I_i(\text{external}) \quad (1)$$

where i, j stand for nearest-neighbour points. V_{ij} is the voltage along the junction, shunted by a resistance R_{ij} , and I_c is the maximum critical current. A_{ij} is the integral of the vector potential along the link between the points i and j . The frustration is defined in terms of the external magnetic field B as $f = BS/\Phi_0$, where S is the surface of the plaquette and Φ_0 the fundamental quantum flux. V_{ij} is given by the Josephson relation

$$\frac{d}{dt}(\Phi_i - \Phi_j) = \frac{2e}{\hbar} V_{ij}. \tag{2}$$

The array is biased by an external current $I_{ext} = I_{dc} + I_{ac} \sin(2\pi \nu t)$. We take it parallel to the y axis. Time is measured in units of the adimensional quantity t/τ , with $\tau = \hbar/(2eI_cR)$. Currents are normalized to I_c .

We have fixed $\nu = 0.1$ and $i_{ac} = I_{ac}/I_c = 1$. The physical quantities have been recorded at the steady state, after a transient time of 1000–2000 τ , and their mean values have been obtained by averaging on 1000–5000 τ , depending on the array size.

3. The dynamical phase space of a locked array

In this section we show that the dynamical states of the array are not unequivocally defined by the voltage value of the Shapiro step. We present a characterization of the different accessible states and discuss their stability against thermal fluctuations and small phase perturbations. Some of the results described in this section have been reported previously in a shorter form [7].

We restrict ourselves to the noticeable case of the first half-integer giant Shapiro step, $\langle V \rangle = 1/2$, with a frustration $f = 1/2$. We consider the cases of arrays with both periodic and free boundary conditions.

According to the current understanding [8, 9] one would expect the dynamics of this locked state to be simply described by the transverse motion (with respect to the direction of the external current) of a checkerboard vortex superlattice, the elementary cell of which consists of 2×2 plaquettes. Consequently, the system is expected to undergo periodic switches between the two degenerate ground states and, when the external current is zero, to exhibit a staircase symmetry: along any staircase definable on the lattice all of the quantities should remain constant (apart from the junctions at the borders). Our numerical simulations confirm these predictions whenever the array is found to lie in the g.s. but they show also that the g.s. is not the only stable dynamical state accessible to the system.

Let us first consider an array with periodic boundary conditions. This is a convenient way to avoid border effects.

Let us consider the plot of $\langle E_{Josephson} \rangle$ versus i_{dc} ($E_{Josephson}$ is defined as the summation over all links of the quantity

$$-(\hbar/2e) J_c \sum_{ij} \cos(\Phi_i - \Phi_j - A_{ij})$$

and the brackets indicate the time averaging). The appearance of a parabola corresponds to that of a Shapiro step in the $\langle V \rangle - I$ characteristic (see figure 1). The curves of figure 1 have been obtained by increasing the value of i_{dc} by steps of 0.01 and restarting the dynamical evolution of the system from the final phase configuration attained with the previous i_{dc} -value. If we repeat the simulation using the same algorithm, but reinitializing the phases at random every time we increment i_{dc} , we observe locking of the array on dynamical states other than the ground state one, characterized by the same value of the Shapiro step voltage but different energies $\langle E_{Josephson} \rangle$. In particular, for $i_{dc} = 0.35$ (a point close to the minimum of the parabola shown in figure 1) we observe the existence of four different

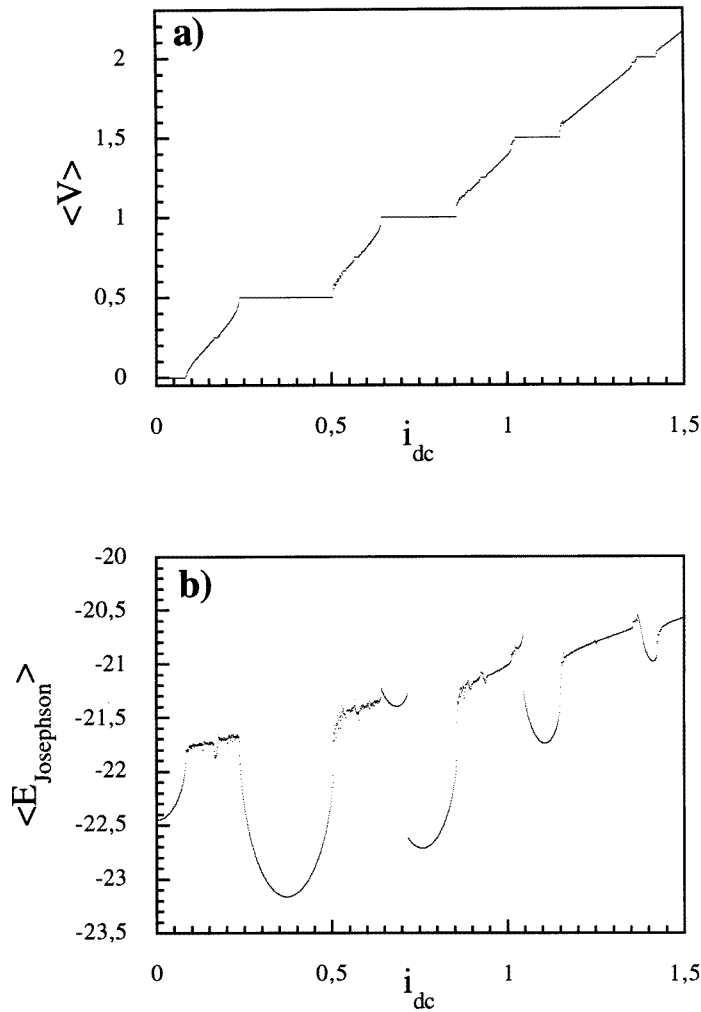


Figure 1. (a) A $\langle V \rangle$ - I_{dc} curve for a 4×4 cell array with $i_{ac} = 1$, $\nu = 0.1$, $f = 0.5$ and periodic boundary conditions. $\langle V \rangle$ has been normalized to $2e/N_y \hbar \omega$, and the currents to J_c . Large Shapiro steps are observable for $\langle V \rangle = 0, 1/2, 1, 3/2$ and 2 . Note also the smaller steps at $\langle V \rangle = 1/4, 3/4$ and $5/4$. (b) An $\langle E_{Josephson} \rangle$ versus I_{dc} plot. $E_{Josephson}$ is defined as $-J_c \sum_{ij} (\cos \Phi_i - \Phi_j - a_{ij})$. The appearance of a parabolic behaviour in this curve mirrors the existence of a plateau in the $\langle V \rangle$ - I plot. Note that at the steps $\langle V \rangle = 1$ and $\langle V \rangle = 3/2$ two different parabolaes are observed. The physical meaning of this is explained in section 3.

accessible dynamical states. Once the system is locked onto one of these four dynamical states, if we increase (decrease) the bias current until the border of the Shapiro step is reached (letting the dynamical evolution restart each time from the phase configuration attained with the previous i_{dc} -value) and we measure $\langle E_{Josephson} \rangle$ for every i_{dc} -value we obtain the four curves shown in figure 2. This numerical protocol corresponds to an experimental one in which the sample is first cooled down below the critical temperature at a fixed i_{dc} and then this latter is continuously increased/decreased until the border of the Shapiro step is reached.

Let us now describe the vortex configurations of these ‘excited’ dynamical states: the

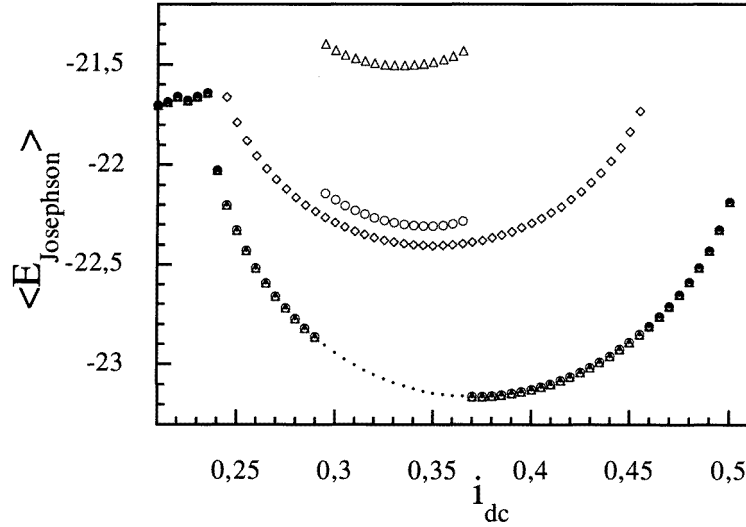


Figure 2. $\langle E_{\text{Josephson}} \rangle$ - i_{dc} curves for a 4×4 cell array with periodic boundary conditions, $f = 0.5$, $i_{\text{dc}} = 1$ and $\nu = 0.1$. To obtain them we first fixed the value of the current i_{dc} (0.35) and then we let the system evolve until it reached its steady state, marked by the measurement of an average voltage value of $1/2$ (V) is given in the same units as for figure 1). According to the initial configuration of the phases four different values of the average energy have been obtained (we represent them respectively by a thick point, a diamond, a circle and a triangle). Starting from each of these four steady-state phase configurations we increased (decreased) i_{dc} towards the borders of the Shapiro step (i.e. $i_{\text{dc}(\min)} = 0.235$ and $i_{\text{dc}(\max)} = 0.503$). For every curve there exist a maximum and a minimum value of i_{dc} between which the dynamical states are stable. For i_{dc} -values outside of the stability range, the system decays onto the curve of minimum energy (which corresponds to the ground state).

vorticity, n , of a plaquette is defined as

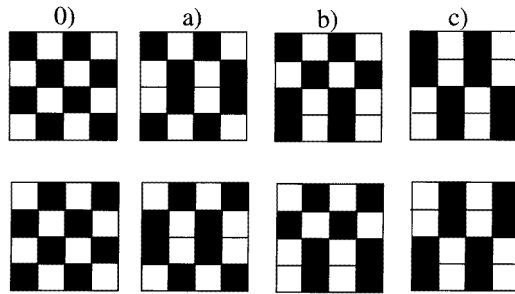
$$n = \frac{1}{2\pi} \sum_{ij} (\Theta_{ij} + A_{ij}) \quad (3)$$

where \sum_{ij} means the anticlockwise sum along the four links ij limiting the cell, and $\Theta_{ij} \equiv \Phi_i - \Phi_j - A_{ij}$ is the gauge-invariant phase taken between $-\pi$ and $+\pi$.

If we apply the vortex definition given in equation (3) to the study of the four different states found at $i_{\text{dc}} = 0.35$ we obtain the images reported in figure 3(a). The four dynamical states can be thus associated, in order of increasing energy, with a checkerboard vortex configuration with: no domain walls (0), one centred domain wall (a), one shifted domain wall (b) or two domain walls (c). It is possible to show that the state with the minimum energy is the one having the expected staircase symmetry [7]. The others containing domain walls are, as far as we are aware, dynamical states that were never observed in previous simulations.

Besides the analysis of their spatial characteristics, a full description of the dynamical states shown in figure 3 requires also a study of their time evolution. All of these dynamical states have been observed in correspondence with the first half-integer Shapiro step; as a consequence they should all be locked states, that is states characterized by a synchronization between the frequency of the external current and some eigenfrequency of the array. To see this explicitly, it is sufficient to look at the currents and at the gauge-invariant phases.

a) Vortex configurations:



b) Cell Currents:

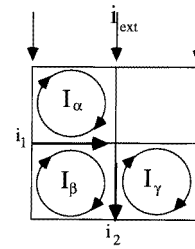


Figure 3. (a) Configurations of vortices observed for the four dynamical states corresponding to the parabola shown in figure 2. We call them (0), (a), (b) and (c) in order of increasing energy. For each state, within a cycle the array oscillates between the two symmetric configurations shown in the diagram. (b) The definition of cell current: if we call I_α , I_β and I_γ the cell currents of the cells α , β and γ , the total current flowing along the horizontal link shared by the cells α and β is given by $i_1 = I_\beta - I_\alpha$, while that flowing in a vertical link (for example, that shared by the cells α and γ) is $i_2 = I_\beta - I_\gamma + i_{external}$.

They turn out both to be periodic with a period twice that of the injected alternating current (i.e. $2T = 2/\nu$).

Figure 4 shows the values of $E_{Josephson}(t)$ and the power supplied to the array by the external current source ($\int \dot{\theta} i_{ext} dt$) [13]. Figures 4(a), 4(b), 4(c) and 4(d) correspond respectively to the states (0), (a), (b) and (c) previously defined.

The main peaks correspond to the sudden ‘switch’ between the two symmetric vortex configurations (see figure 3(a)), which is the displacement by one cell of the superarray of vortices. It takes the system a time $T = 1/\nu$ to ‘switch’ between these states, and $2T$ to turn back to the initial one.

As we go from 4(a) to 4(d) we observe an increase of the power level needed to operate the ‘switching’, an increase of the average quantity $\langle E_{Josephson} \rangle$ and a reduction of the distance between the highest and lowest values of $E_{Josephson}$.

The sudden ‘switch’ between the two complementary vortex configurations is only a consequence of the vortex definition given in (3).

Actually the displacement of a vortex (and thus of the whole vortex superarray) is a continuous process that implies a continuous decrease of the cell current intensity in the J -cell and a simultaneous continuous increase of the intensity of the cell current intensity in the $(J + 1)$ -cell (the cell currents are defined in figure 3(b)).

The current density is transferred from one cell to the next through the shunt resistances. For a while, during this process of transfer, the array shows a very low magnetic contrast (intuitively we relate the magnetic contrast to the difference between the value of the cell current of a plaquette ‘containing’ a vortex and that of an ‘empty’ one), and $E_{Josephson}$ and the external power reach a maximum. When $E_{Josephson}$ and the external power are round a minimum, the cell current distribution shows clearly defined peaks at the cells where vortices are placed; at these values of the time the magnetic contrast is a maximum. The difference between the maximum and minimum $E_{Josephson}$ -values reduces in going from figure 4(a) to 4(d). This suggests (as we will check soon) a simultaneous decrease of the stability of the vortex configurations.

While the ground state is by definition a stable dynamical state we do not know anything

about the stability of the excited dynamical states, so we have to study it.

As a first step we have considered the effect of the temperature. Temperature fluctuations may cause the erasing of some dynamical attractors [14], and one may wonder whether or not this is the case for the states that we have observed at $T = 0$. The effect of the temperature on equation (1) can be taken into account by adding a white-noise current term, n_{ij} , such that [15]

$$\langle n_{ij}(t) \rangle = 0 \tag{4}$$

and

$$\langle n_{ij}(t + \tau)n_{kl}(t) \rangle = \frac{2k_B T}{R_{ij}} \delta(\tau)\delta_{ij,kl} \tag{5}$$

where $\langle \rangle$ represents the ensemble average.

We observed that the dynamical states considered here survive, at least up to a noise-equivalent temperature of $KT/J = 10^{-2}$ (see figure 5). Above this temperature, Shapiro steps become unstable and disappear.

Another important point to check is the stability of the solutions against small perturbations. To do this we considered Floquet's exponents [16].

For a given phase configuration of the system, represented by the vector $\Phi \equiv \{\phi_0, \phi_1, \dots, \phi_{N-1}\}$, a periodic solution with period T has to satisfy the following condition: $\Phi(T) = \Phi(0)$. If one adds a perturbation to the initial configuration, $\Phi(0) \rightarrow \Phi(0) + \delta\Phi(0)$

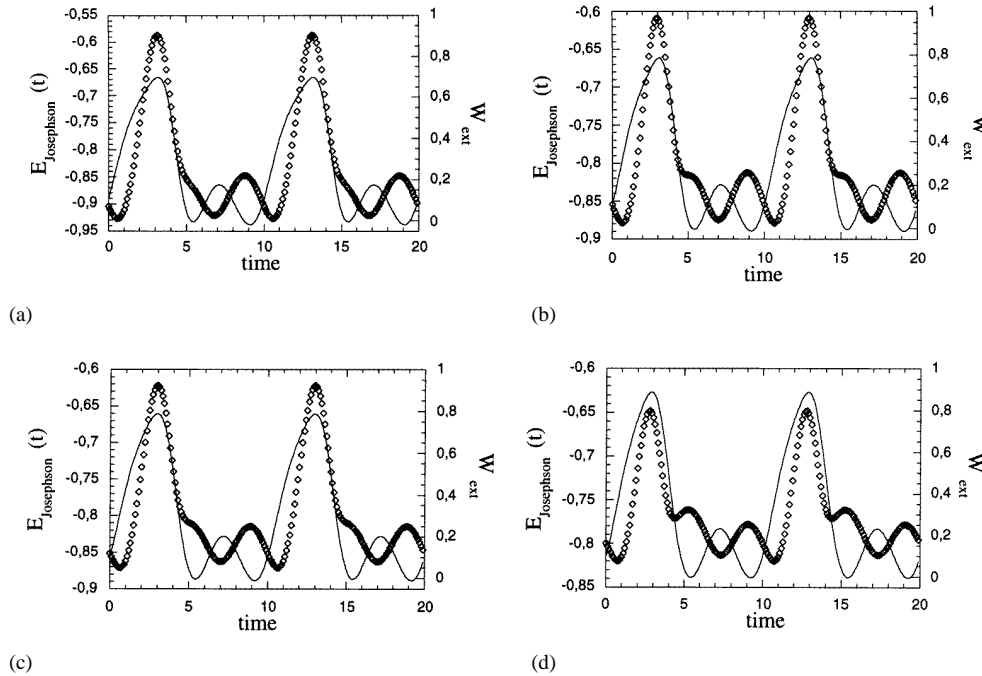


Figure 4. Time evolution of the Josephson energy (\diamond), and of the power supplied by the external current source (the continuous curve): $\dot{\theta}i_{e,xt}$ (where θ is the phase difference between the first and last rows of the array). The curves (a), (b), (c) and (d) (ordered from left to right, top to bottom) refer respectively to the dynamical states (0), (a), (b) and (c) shown in the previous figure. Energies are given in units of $J_c\hbar/(2e)$, and normalized to the number of links in the array.

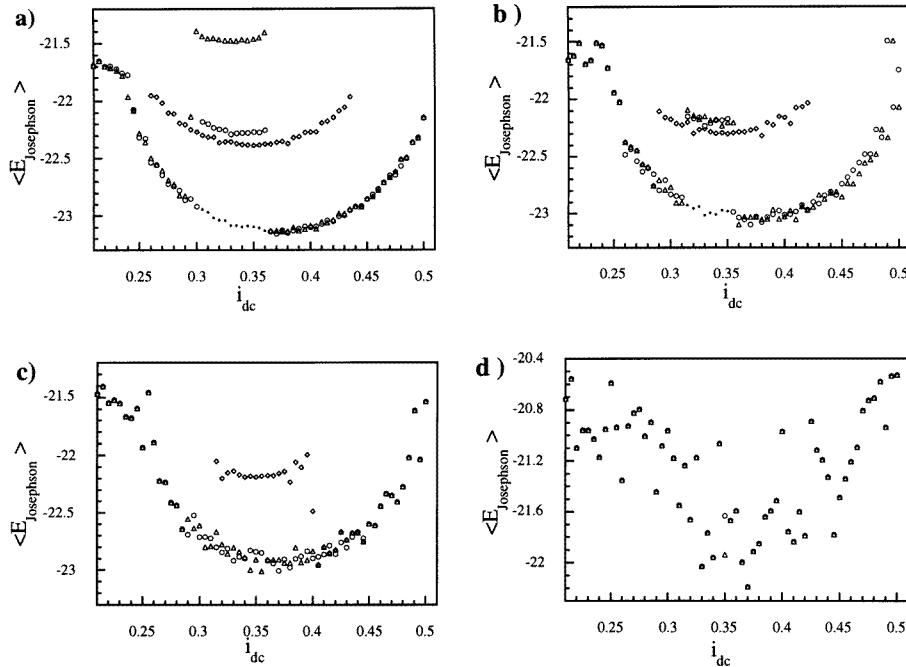


Figure 5. Energy curves obtained under the same conditions as for figure 2 but with an increasing value of the reduced temperature T^* : 0.001, 0.005, 0.01 and 0.05 (from left to right and from top to bottom). T^* is related to the dimensional temperature, T , by $T^* = ek_B T / \hbar J_c$. As we raise T^* the parabola with higher energy become unstable and disappear.

and $\Phi(T) \rightarrow \Phi(T) + \delta\Phi(T)$. If $\delta\Phi$ is small enough we can linearize around $\Phi(0)$ obtaining $\delta\Phi(T) = M \delta\Phi(0)$, where M is an $N \times N$ matrix. Let us now calculate the eigenvalues of M . If their moduli are all smaller than 1, after a sufficiently long time $\delta\Phi$ will tend to 0; that is, the system will return to the initial state. However, if at least one eigenvalue has a modulus greater than 1 the evolution of the perturbed system will separate further and further from that of the non-perturbed one. Equivalently, if we define the eigenvalues of the matrix as $\lambda_i = \exp(x_i)$, having a stable solution requires all the real parts of the exponents x_i to be negative. In figure 6 we show the values of the real parts of the exponents x_i obtained for all of the dynamical states whose energy is plotted in figure 2. We conclude that all of the dynamical states (ground state and excited states) are stable against a phase perturbation within the i_{dc} -ranges where we observed a locked dynamics.

An analogous behaviour is found in arrays with free boundary conditions (fbc). Again we find four different stable states with zero, one and two domain walls. The main difference from the case of arrays with periodic boundary conditions (pbc) is the shrinking of the range of i_{dc} -values where a clear magnetic contrast is observed. This fact must be taken into account when an experiment on small-size systems is performed.

4. The relevance of the geometry and the size of the arrays

We now turn to the following two questions. To what extent can we scale down the system and still observe the properties found in large 2D arrays? What is the influence of the size

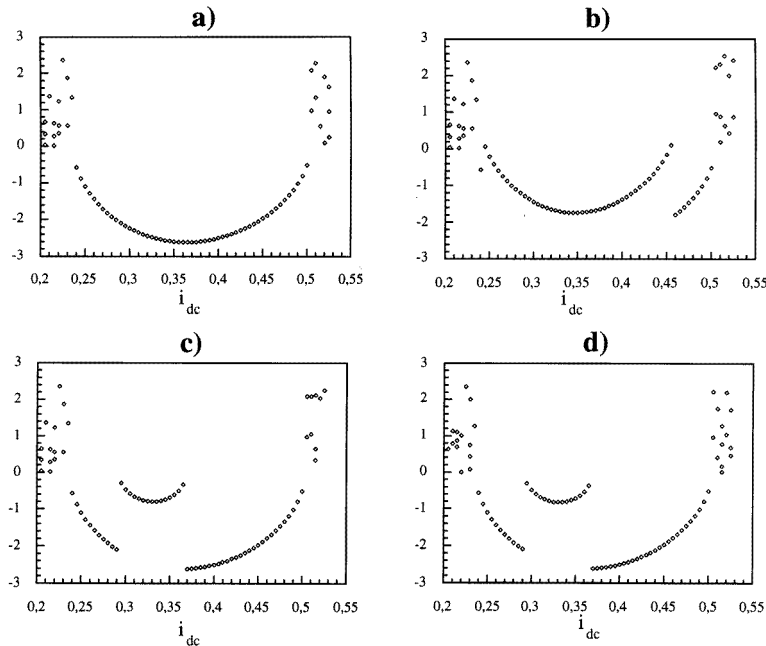


Figure 6. A study of the stability of the dynamical states (0), (a), (b) and (c) (respectively (a), (b), (c), (d)). We plot the values of the Floquet exponents that represent the eigenvalues of the matrix M obtained, after one period, by linearizing the phase perturbation to the periodic solution. A state is stable against perturbations if the modulus of every eigenvalue is smaller than 1 (exponent smaller than 0); every eigenvalue that does not fulfil the previous condition corresponds to a direction of instability in the space of configurations. For each i_{dc} -value we show all the exponents greater than 0 and, by default, the greatest exponent.

and of the geometry of the lattice on the appearance of the domain walls?

In order to answer these questions we decided, as a first step, to investigate the dynamics of both horizontal and vertical ladders of different size, all subjected to a frustration, f .

Let us consider first horizontal ladders (arrays with $N \times 2$ sites). For a frustration $f = 1/q$, where q is an integer number, the smallest ladder commensurable with f is the one composed of q plaquettes. Let us impose periodic boundary conditions in order to simulate an infinite ladder. Under these conditions we observe, as expected, only SSS with $\langle V \rangle = n/q$.

If we take ladders with free boundary conditions, still commensurable with f , we observe the coexistence of n/r ($r \neq q$) and n/q steps. As $N \rightarrow \infty$ the behaviour of the system tends to that of the infinite ladder array, and the non-commensurable SSS become narrower and narrower. For ladders with a number of plaquettes different from nq , we observe both kinds of SSS, and the non-commensurable ones survive even for very large arrays.

All of the above dynamical states, and in particular those observed when $f = 0.5$, are characterized by a single-valued $\langle E_{Josephson} \rangle$ versus i_{dc} curve.

To sum up, the width of a ladder (and thus of a 2D array) induces a selection among the allowed locked dynamical states, SS, and regulates the extension of their attraction basins. The dynamical evolution of a locked state is characterized by the periodic displacement of the vortex superlattice. We have found no evidence of the existence of locked states

exhibiting domain walls in the steady state. Domain walls that may be induced by the choice of the initial conditions, subjected to the Lorentz force due to the bias current, move with the vortex and annihilate when they reach the border. Only in the case of periodic boundary conditions are these defects re-injected into the ladder, and this may affect the locking.

Let us now turn our attention to ladders parallel to the direction of the bias current (e.g. vertical ones).

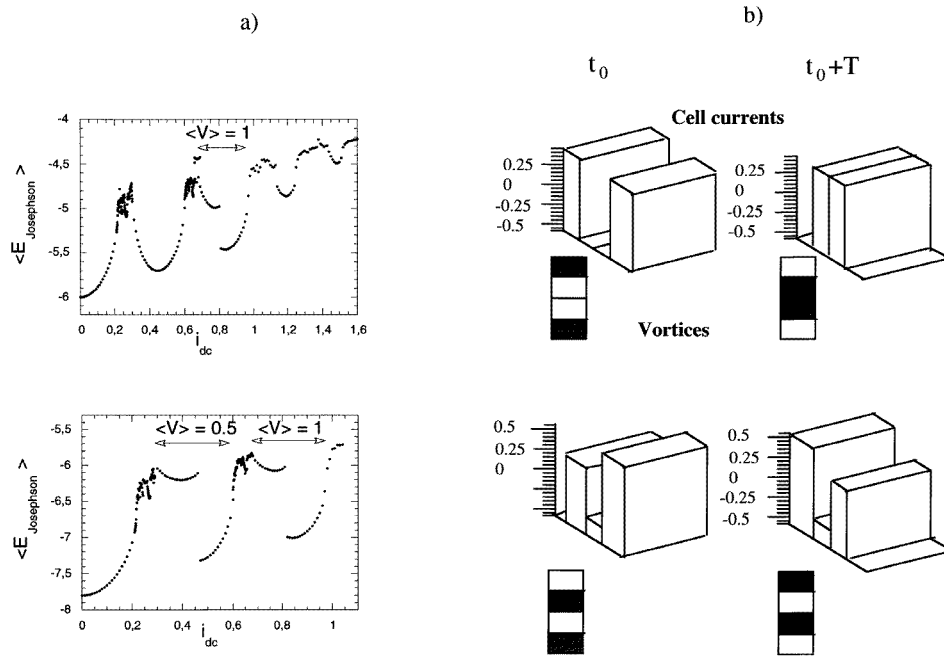


Figure 7. $\langle E_{Josephson} \rangle - I_{dc}$ curves obtained for vertical ladders, with three (top left) and four (bottom left) cells. As shown by the diagram, the dynamical states accessible to the system are not unequivocally determined (see the jumps observed in the correspondence of the $\langle V \rangle = 1$ SS for the three-cell ladder, and of the $\langle V \rangle = 1/2$ and $\langle V \rangle = 1$ SSs for the four-cell one). In (b) we show the cell currents and the positions of the vortices for two distinct dynamical states accessible to the four-cell array at $i_{dc} = 0.5$ and $\langle V \rangle = 1/2$. The state containing the domain wall (top) corresponds to the parabola with the highest energy. At t_0 , $\langle E_{Josephson} \rangle$ and the external power are in the neighbourhood of a minimum.

Figure 7(a) shows that even for ladders constituted of as few as four cells the $\langle E_{Josephson} \rangle - i_{dc}$ curve shows features very similar to those we observed for 2D arrays. Indeed, in the case of such a simple system we also observe a jump between two different parabolae. If we concentrate on the half-integer SS and we pick up a vortex view of the two dynamical states accessible to the four-cell ladder on the half-integer SS we obtain the configurations plotted in figure 7(b). This figure demonstrates that the dynamical configuration of a JJ array locked on certain Shapiro steps is not unique for all of the systems having a minimum finite extension along the direction of the external current. The minimum extension of the ladder for which we have observed the formation of the domain walls is three cells.

5. Conclusions

We have clearly shown that the existence of a Shapiro step does not determine unequivocally the locked dynamical state of a JJA.

A full description of the dynamics can be obtained only by measuring average quantities like $\langle E_{Josephson} \rangle$ as function of i_{dc} and by monitoring the dynamical evolution of the vortex configuration.

Between the various dynamical states accessible to the systems, the one with the lowest energy always coincides with the ground state described in many previous papers. The others represent dynamical solutions, exhibiting one or more domain walls.

These excited states are stable against small temperature and phase fluctuations.

The discovery of such excited dynamical states may be relevant for the interpretation of experiments that aim to investigate the array dynamics on a microscopic scale [17]. Moreover, they may help in understanding why it is not easy to produce coherent 2D JJ microwave emitters and detectors. Indeed, as for the static case [18], it seems to us very improbable that a fully developed ground state could be attainable over the whole sample. Domain walls may easily develop. They may certainly derive from intrinsic defects of the sample but, as we have shown in this paper, they can form even in perfect samples, depending on the experimental conditions under which the measurement is performed. As an example, a relevant role may be played by the dimension of the sample, its shape, and, finally, the boundary conditions; indeed we observed rather different dynamical behaviour of the sample with fbc and the sample with pbc. Other important factors may include the cooling rate and the stray field at the transition temperature: they determine the freezing configuration of the phases.

To understand the origin of the dynamical behaviour of a JJ array we have turned our attention to much simpler systems, such as JJ ladders.

The horizontal extent of the ladders, in conjunction with the frustration, controls the selection and the width of the SS, but it has no influence on the generation of excited dynamical states with domain walls.

The fact of the dynamical states and the domain wall formation being unequivocal, on the other hand, is strictly connected to the vertical extension of the ladders. We have shown that excited dynamical states can be found also in very short ladders (three or four cells long).

Acknowledgment

We acknowledge financial support provided by the EEC under contract CHRX-CT92-0068.

References

- [1] Clark T D 1973 *Phys. Rev. B* **137** 137
Leemann C, Lerch P and Martinoli P 1984 *Physica B* **126** 475
- [2] Benz S P, Rzchowski M S, Tinkham M and Lobb C J 1990 *Phys. Rev. Lett.* **64** 693
- [3] Lee C H, Newrock R S, Mast D B, Hebboul S E, Garland J C and Lobb C J 1991 *Phys. Rev. B* **44** 921
Hebboul S E and Garland J C 1991 *Phys. Rev. B* **43** 13 703; 1993 *Phys. Rev. B* **47** 5190
Octavio M, Free J U, Benz S P, Newrock R S, Mart D B and Lobb C J 1991 *Phys. Rev. B* **44** 4601
- [4] Bohr T, Bak P and Jensen M H 1984 *Phys. Rev. A* **4** 1970
- [5] Giannelli A, Ritort F and Giovannella C 1995 *Europhys. Lett.* **29** 419
- [6] Domínguez D, José J V, Karma A and Wiecko C 1991 *Phys. Rev. Lett.* **67** 2367
Domínguez D and José J V 1994 *Int. J. Mod. Phys. B* **8** 3749

- [7] Ciria J C and Giovannella C 1994 *Proc. 7th Int. Symp. on Weak Superconductivity (Smolenice)* ed Š Beňačka, P Seidel and V Štrbík (Bratislava: IEEASAS) p 324; 1995 *Nonlinear Superconducting Devices and High- T_c Materials* ed R D Parmentier and N F Pedersen (Singapore: World Scientific)
- [8] Free J U, Benz S P, Newrock R S, Mart D B, Lobb C J and Octavio M 1990 *Phys. Rev. B* **41** 7267
- [9] Lee K H, Stroud D and Chung J S 1990 *Phys. Rev. Lett.* **64** 692
Lee K H and Stroud D 1991 *Phys. Rev. Lett.* **43** 5280
- [10] Kim J and Lee H C 1993 *Phys. Rev. B* **47** 582
- [11] Lee H C, Newrock R S, Mast D B, Hebboul S E, Garland J C and Lobb C J 1991 *Phys. Rev. B* **44** 921
Yu W, Harris E B, Hebboul S E, Garland J C and Stroud D 1992 *Phys. Rev. B* **45** 12624
- [12] Mon K K and Teitel S 1989 *Phys. Rev. Lett.* **62** 673
Chung J S, Lee K H and Stroud D 1989 *Phys. Rev. B* **40** 6570
- [13] We can assign to a 2D array of Josephson junctions a Hamiltonian:

$$H = -J_c \sum_{ij} \cos(\Phi_i - \Phi_j - a_{ij}) - \sum_i \int \dot{\theta} i_{ext} dt.$$

See, for example,

- Choi M Y and Kim S 1993 *Proc. 2nd CTP Workshop on Statistical Physics: KT Transitions and Superconducting Arrays (Seoul)* ed D Kim, J Chung and M Y Choi (Seoul: Min Eum Sa)
- [14] Eikmans H and Van Himbergen J E 1991 *Phys. Rev. B* **44** 6937
- [15] Ambegaokar V and Halperin B I 1969 *Phys. Rev. Lett.* **22** 1364
- [16] See, for example,
Ott E 1993 *Chaos in Dynamical States* (Cambridge: Cambridge University Press)
- [17] Booi P A A, Benz S P, Doderer T, Hoffmann D, Huebener R P and Lachenmann S G 1994 *Phys. Rev. B* **50** 3158
- [18] Runge K and Pannetier B 1993 *Europhys. Lett.* **B 44** 737 and references therein